Optical Materials, Volume 20, Issue 4, November-December 2002, Pages 283-294.

AFM observation of surface topography of fibre Bragg gratings fabricated in germanium-boron codoped fibres and hydrogen-loaded fibres

C Y Wei[a*], C C Ye[b], S W James[b], P E Irving[a] and R P Tatam[b]

a Damage Tolerance Group, School of Industrial and Manufacturing Science, Cranfield University, Cranfield, Bedford MK43 0AL, UK

b Optical Sensors Group, Centre for Photonics and Optical Engineering, School of Engineering, Cranfield University, Cranfield, Bedford MK43 0AL, UK

ABSTRACT

This paper reports the measurement of the surface topology of optical fibres containing a fibre Bragg grating (FBG) using an Atomic Force Microscope (AFM). The AFM observation was made on FBGs fabricated via the phase mask technique in germanium-boron codoped optical fibres, in hydrogen-loaded germanium-boron codoped fibres and in standard telecommunications optical fibres. The surface images reveal that a spatial corrugation pattern was induced by the UV-irradiation, with a period that is half of the period of the phase mask. This UV-induced surface structure was found only on the side of the fibre facing towards the incident UV irradiation and did not appear on the rear surface. The AFM probe scanned a 10×10 μm surface area at seven sites along the 6.0 mm length of fibre that was exposed to the UV irradiation. The amplitude of the spatial corrugation pattern observed on the AFM image was quantified for each site. It was found that the amplitude in a range of 0.7-3.2 nm was a function of UV-laser intensity distribution and the type of fibre. Hydrogen loaded optical fibres exhibited a corrugation with an amplitude twice as large as that observed in the Ge-B-doped

* Correspondence author: Building 40, SIMS, Cranfield University, Bedford MK43 0AL, UK.
E-mail: c.wei@cranfield.ac.uk; fax: +44 1234 754129; tel: +44 1234 750111 ext. 2464

fibres that were not hydrogen loaded. This correlates with the increase in photosensitivity produced by the hydrogen loading. A similar UV-induced spatial corrugation was also observed on standard telecom fibres, but without inducing the refractive index change in the fibre core. The observation of surface topology provides an insight into the structural changes induced during FBG fabrication. UV-induced densification and laser ablation could account for the formation of the surface troughs.

PACS codes: 42.70a; 42.79 Dj; 68.37.Ps

Keywords: Photosensitivity of fibre Bragg gratings; AFM observation of fibre Bragg gratings, Hydrogen loaded optical fibres; Surface topography of fibre Bragg gratings; Surface modulation of fibre Bragg gratings

1 INTRODUCTION

Since their discovery in 1978 [1], fibre Bragg gratings (FBGs) have found applications in optical fibre sensing and telecommunications systems. A FBG is an UV induced periodic perturbation of the refractive index of the core of an optical fibre. Photosensitivity refers to the tendency of a material to suffer a permanent change in refractive index or opacity induced upon exposure to light. The magnitude of the photosensitivity gives an indication of the amplitude of the refractive index change that may be induced. The photosensitivity of optical fibres is enhanced either by doping the fibre core with elements such as Ge, or Sn, or by soaking the fibre in a high pressure hydrogen atmosphere for a number of days. One of the commonly used core dopants is germanium. The high pressure hydrogen-loading technique has been recognised as an efficient means of achieving ultrahigh photosensitivity in GeO_2-doped fibres [2]. Hydrogen loading is also a common method used to allow FBGs to be fabricated in fibres such as standard telecommunication fibres, which have a low germanium content.

A full understanding of the factors that contribute to the photosensitivity, and of the reasons why

hydrogen loading increases the magnitude of the refractive index change that may be induced by UV irradiation, has not been reached. A number of theories have been proposed based on observations and assumptions. Two principal mechanisms are claimed: structural densification and colour centre formation [3]. UV-induced densification has been proposed by several investigators to account for the formation of FBGs in Ge doped fibres [4, 5]. In such germanosilicate optical fibres, a structural change of the glass in the fibre core into a more compact configuration has been observed using transmission electron microscopy (TEM) [6]. Periodically spaced dark fringes in the core of tin doped germanosilicate fibre were observed in a thin film obtained by grinding and polishing the fibre. These dark regions were believed to be composed of dense regions of glass which were induced at the location of the bright UV fringes. However no such pattern was observed in the FBGs fabricated in hydrogenated fibres using TEM [7]. Based on this investigation, it was suggested that the UV induced densification could account for a large part of the refractive index modulation induced in rare earth element-doped fibres, but that it was not applicable to the hydrogen loaded germanosilicate fibres. This suggests that a different mechanism is responsible for the formation of FBGs in hydrogen loaded fibres.

Two theories have been proposed to explain the photosensitivity increase caused by hydrogen loading. Firstly a colour centre model has been suggested to account for the photosensitivity of hydrogen loaded fibres [7]. In the model, UV light photoionizes some bleachable defects of the germanosilicate glass. Electrons released from these defects are free to move to other defect sites. The resultant refractive index change is linked simply to the photoinduced change in absorption through the Kramers-Kronig relationship. Secondly, it has been proposed that a chemical reaction takes place in the presence of hydrogen [8]. In hydrogenated fibres an increase of absorption loss at the first overtone of the O-H vibration at a wavelength of 1.27μm is observed over a period of time [9]. This observation is attributed to the reaction of the hydrogen with oxygen to form hydroxyl ions. The formation of a hydroxyl group changes the refractive index. In addition, in hydrogen loaded germanosilicate fibres,

the reaction between Ge-ions and hydrogen forms GeH, changing the band structure in the UV. These changes influence the local refractive index according to the Kramers-Kronig model. Kashyap [10] stated that all three mechanisms could prevail in optical fibres. The contribution of each mechanism depends on the type of optical fibre and photosensitisation process.

Changes in the surface topology of optical fibres associated with UV induced refractive index changes have not been revealed previously directly under microscopic observation. Poumellec et al [5] first used the Atomic Force Microscopy (AFM) technique to observe surface modulation on slices of Ge:SiO_2 preforms following grating inscription. However, due to the restrictions of the technique at that time, this investigation was made on planar slices of material rather than on optical fibres. The slices were comprised of a SiO_2 cladding doped with B_2O_3 and P_2O_5 deposited upon a GeO_2-doped core. A surface corrugation pattern was observed following the inscription of FBGs in the slices, from which the densification mechanism was determined to be responsible for the photosensitivity. The investigation reported here explores the structural change induced on the primary optical fibre surface by UV irradiation. The surface topology of Ge-B-doped fibres and hydrogen loaded fibres are compared.

2 FIBRE BRAGG GRATING FABRICATION PROCESS

2.1 Optical fibres and the hydrogen loading process

The investigation was carried out using two types of fibres: standard telecommunication fibres (SM-1322/P3022-E, supplied by Optical Fibres, Deeside) and germanium-boron-codoped fibres (Fibercore PS1250). Fibrecore PS1250 optical fibre is composed of a silica cladding and a core of 5% wt germania with boron phosphorus doped-silica to enhance the photosensitivity. Both types of fibres are single-mode with a 125 μm diameter cladding and a polyacrylate coating with a cut-off wavelength of 1250nm. Prior to the inscription of FBGs, samples of the Ge-B codoped fibres were placed in a

hydrogen chamber at 120 bars for seven days at 25°C, while the standard telecommunication fibres experienced hydrogen-loading at 135 bars for 9 days, also at 25°C. Both hydrogen loaded and non-hydrogen loaded fibres were used for FBG inscription.

The polyacrylate buffer coating exhibits a large absorption in the UV, requiring its removal prior to UV irradiation of the fibre. The fibres were soaked in a proprietary paint-remover to remove a 20 mm long section of the polyacrylate coating, and a lens tissue soaked with acetone was used to remove the residual coating.

2.2 UV-irradiation process and AFM observation

An injection seeded frequency quadrupled Nd:YAG laser operating at 266 nm with a pulse width of 5 ns and 10 Hz repitition rate was used to fabricate the FBGs. The FBGs were fabricated in the stripped section of the fibres using a phase mask configuration [11], as shown in Fig. 1. The period of the phase mask was 910nm and the Bragg wavelength of the FBGs was 1320 nm. The exposure time for each FBG was 60 s.

Four different exposure regimes were exploited to examine the influence of the laser energy on surface changes caused by the exposure. A cylindrical lens was used to produce a line focus parallel to the axis of the fibre, and the laser energy was controlled to produce average pulse intensities of 2.0, 2.4, 2.8 and 3.2 W/cm^2. The side of the fibre that faced the UV beam was carefully marked. The location of the exposure centre and the 6mm long exposure region were also marked. Hydrogen loading the photosensitive fibre had the effect of increasing the reflectivity from 27% to 60% when the FBGs were inscribed under an average intensity of 2.4 W/cm^2 for 60s. Under the same exposure condition, the FBGs written in hydrogen-loaded standard telecom fibres had a similar reflectivity as the

photosensitive fibres. However, the FBGs in non-hydrogen loaded telecom fibres were so weak that the reflectivity was not measurable.

The AFM technique examines the surface topography of an object through a fine ceramic or semiconductor tip scanning over a surface. The tip is positioned at the end of a cantilever beam. As the tip is repelled by or attracted to the surface, the cantilever beam deflects. The magnitude of the deflection is detected using a laser. The detected signal is amplified by a lock-in amplifier, and then converted into a vertical deflection using the z-axis sensitivity of the AFM. A plot of the laser deflection versus tip position on the sample surface provides the surface topography with peaks and troughs.

The AFM observation was performed using a Digital Instruments Dimension^{TM} 3000 SPM under tapping mode in which the tip taps across the surface at a frequency of 1 Hz. The advantage of using tapping mode is that the lateral forces are virtually eliminated, so there was no scraping of the surface under the probe tip. The tip scanned an area of 10×10 μm^2 on the surface of the fibre. The AFM scanning was performed on fibre samples prepared as detailed in Table 1. For the FBGs fabricated in Ge-B codoped fibres with and without hydrogen loading under 2.0 W/cm^2 exposure, the AFM observation was conducted at the location of the centre of the UV exposure, and repeated at positions ±1 mm, ±2 mm, and ±3 mm away from the central exposure point.

3 AFM SURFACE IMAGES

3.1 Comparison of surface images of the UV-irradiated surface with those of non-UV-irradiated surface

The AFM images revealed that the UV-exposure produced a spatially periodic surface relief pattern on

the exposure surface (surface facing the UV beams during fabrication) for all types of fibres. Figure 2 shows the pattern that appeared on the photosensitive fibres which were exposed to UV radiation at an average intensity of 2.4 W/cm^2. The bright stripes on the 2-D image (Fig. 2b) correspond to the peaks of the surface relief pattern while the dark areas correspond to the troughs (or valleys). This periodic pattern can be seen clearly in the 3-D image (Fig. 2 c). The white spots observed in Fig. 2b, are probably caused by the natural surface coarseness and debris left on the fibre surface by the stripping of the buffer coating. Taking a line across the 2-D surface (Fig. 2b), allows the vertical profile to be displayed as shown in Figure 2a. The cross-section roughness spectrum exhibits peaks and troughs aligned with the axial direction of the fibres. The amplitude of the corrugation is defined as the vertical distance from the minima of the troughs to the surface level that excludes features attributed to surface contamination which is shown as the hills above the surface level, as seen in Fig. 2a. The average period of the relief pattern determined from the AFM images was 455 nm, which is equal to the period of the interference fringes generated by the phase mask. This value is in agreement with the period of the Bragg gratings formed in the fibre core, which gives the Bragg wavelength of 1320nm. The surface relief pattern period indicates that the surface troughs are the location of the bright interference fringes and that the horizontal level of the surface peaks is the surface level prior to irradiation. The energy of the UV irradiation appears to alter the topography of the pristine glass.

The 2-D and 3-D images obtained from a region on the surface of the optical fibre that had not been UV irradiated are shown in Fig. 3. When the observation was made on the region outside of the 6.0 mm irradiated section, there is no sign of the periodic pattern observed in Figure 2. The 3-D image shows the surface roughness with a number of peaks associated with surface contamination. The cross-section roughness analysis in Fig. 3a indicates a 0.7 nm vertical distance from the peaks to the troughs of the natural surface roughness, which is half of the value seen following irradiation.

Figure 4 shows an AFM image of a section of fibre lying within the irradiated region, but facing away from the incident UV beams. No corrugation pattern is observed on the rear surface of the FBGs, though a number of the irradiated fibres were examined using AFM. The UV-irradiation had no influence on the rear surface of the fibre. This is due to the reduction of UV power intensity through the silica glass. The UV intensity was measured along the beam profile width at the position where was behind the rear surface of the fibre. The measurement was repeated at the same position when the fibre was removed. Figure 5 shows the UV intensity distribution in these two cases. The U-shape in the distribution curve with the presence of a fibre indicates that a large quantity of UV energy was absorbed by the fibre. Upto 22% UV intensity remained at the central location of the fibre. This implies that the UV interference fringes that reach the rear surface possess only 22% energy which is below the intensity required to alter the surface topography.

These observations reveal that the surface morphology of the irradiated sections containing FBGs is not symmetrical. The asymmetrical structure may have an impact on the optical and mechanical performance of the FBG. The mechanical strength of the fibre has been shown previously to be reduced following UV-irradiation [12, 13]. In Cordier's work [6], following grating inscription, microcracks running between the dark and light regions were evident in preform slices which were ion-milled for TEM observation. The fringes of the gratings appear as the dark band in the TEM images as a result of structural densification. Stress concentrations may exist in the interface between the valley and peak of the surface relief pattern that could lead to the initiation of cracks, resulting in a low failure stress.

3.2 Amplitude of the surface relief pattern for different regions of the UV-irradiated section

These observations were conducted on the Ge-B codoped fibres in hydrogen-loaded and non hydrogen-loaded conditions. Both fibres were exposed using an average intensity of 2.0 W/cm^2. The AFM probe

scanned a 10×10 μm^2 area at 1.0 mm intervals from the beginning of a 6.0 mm long irradiated section. The 2-D surface images obtained are shown in Figures 6 and 7. Each figure contains 4 images representing the observed area at the centre of the irradiated region and at positions 1 mm, 2 mm and 3 mm away from the centre.

Figure 8 shows the amplitude of the surface relief pattern as a function of the position of the irradiated region. The amplitude decreases away from the centre of the irradiated region, with the highest value located at the centre of the region. In Fig. 8, the UV beam profile shows the intensity distribution along the irradiated region. For both fibres, the change of the surface relief amplitude with distance matches the spatial distribution of the intensity of the UV irradiation. The UV-intensity distribution follows a Gaussian profile with a full width half maximum of 6.0 mm. The AFM observed that the surface relief appeared within the 6.0mm central region of the irradiated area. In Fig. 8, it can be seen that the UV intensity decreases to 50% of its peak value when the position is 3.0 mm away from the irradiated centre. The UV interference fringes outside of the 6.0 mm central region had inadequate power to create the surface modulation. Thus, the intensity of the laser energy has a direct impact on the formation of the surface troughs. There is a direct correlation between the intensity of the UV irradiation and the amplitude of the surface relief pattern. Hydrogen loading the optical fibres appears to magnify the effect, leading to an increase in the amplitude of the surface relief pattern. As shown in Figure 8, the amplitude of the UV-induced corrugation on the hydrogen loaded photosensitive fibres double the value measured on the non-hydrogen loaded fibres.

3.3 Amplitude of surface relief pattern for different types of fibres and laser pulse energy

To compare the difference of the surface relief pattern in different types of fibres under different laser pulse energies, the measurements were made at the centre of the exposure region for all the fibres.

Regardless of the type of fibre, all irradiated surfaces show a corrugation pattern with the same period (455 nm). Fig. 9 shows the irradiated surface of a standard telecom fibre. A periodic pattern with a 1.91 nm amplitude is clearly seen. Standard telecom fibres have little photosensitivity to form FBGs. The UV-induced pattern observed in this case suggests that no direct link exists between the surface relief and the change of refractive index in the fibre core.

Figure 10 shows the amplitude of the surface relief pattern measured from AFM images of four types of fibres which were exposed to different levels of laser power. There are two significant observations that can be made. Firstly, for the same type of fibre, the surface relief amplitude is a function of the laser power. In the Ge-B codoped fibres, the amplitude increases from 1.24 to 2.09 nm when the average pulse density rises from 2.0 to 2.8 W/cm^2. The standard telecom fibres show a similar trend, the amplitude increasing from 1.91 to 3.14 nm as the laser power raised from 2.4 to 3.2 W/cm^2. This is consistent with the data in Fig. 8 where the amplitude of the surface pattern was strongly correlated to the distribution of laser power within the irradiated region.

Secondly, the irradiated surface of both standard telecom and photosensitive fibres which were hydrogen-loaded demonstrates a larger surface relief amplitude than that observed on the fibres that were not hydrogen loaded. Under the same exposure parameters, the amplitude of hydrogenated standard telecom fibres is 2.4 nm, which is 25% higher than that observed on the non-hydrogenated fibres. Hydrogen loading the photosensitive fibres enhances the amplitude of the surface relief pattern over 100% compared to the non-hydrogenated photosensitive fibres.

4 MECHANISMS FOR THE FORMATION OF SURFACE RELIEF PATTERNS

The AFM observations show that the spatially modulated UV irradiation alters the surface topography

of glass fibre, resulting in a periodic pattern with a series of peaks and troughs. The pattern observed on the standard telecom fibres, which is known to have low photosensitivity, indicates that the surface change may not be linked to the formation of FBGs in the fibre core. However, hydrogen loading enlarges the magnitude of the surface relief pattern as well as increasing the photosensitivity. The surface relief period closely matches the FBG period. It is not clear whether the surface structure change interferes with the change in the fibre core during the FBG inscription.

A consideration of the thermal decay phenomena [14] may aid the understanding of this issue. The thermal decay of a FBG describes the phenomena of the reversal of the change in refractive index at elevated temperature. The thermal degradation of the refractive index modulation results in a reduction in the peak reflectivity and a small reduction in bandwidth of the FBG. It was observed that the decay of FBGs fabricated in hydrogen loaded fibres is more significant than that of FBGs fabricated in fibres that were not hydrogen loaded.

Two mechanisms have been proposed to explain the thermal reversal of the refractive index modulation. The first is associated with an activation barrier E_{a1}[15]. With thermal assistance, the UV induced defect overcomes the activation energy barrier, with the result that its contribution to the modulation is reduced, and grating decay occurs. Corresponding to this theory is the colour centre mechanism that electrons in glass are displaced and trapped in the modulation sites. At elevated temperatures, these electrons are released and reversed, resulting in the thermal decay phenomenon. The second theory is associated with densification mechanisms. Douay et al [7] observed that the amplitude of the surface relief pattern in a non-hydrogen loaded boron co-doped germanosilicate preform slice decreased, eventually becoming too low to measure, when the slice had been annealed at 650°C. The disappearance of the surface relief, correlated with the reduction of the reflectivity of the FBGs, appears to support the densification model. This observation indicated that the surface relief

pattern is responsible for the refractive index modulation. This pattern could be reversed at an elevated temperature that may relax the glass structure. However, the same investigators did not find the periodically dark regions in the core of hydrogen-loaded fibres from their TEM observation, which seems not to support the densification theory associated with hydrogen-loaded fibres.

The thermally induced decrease of the refractive index modulation of the core has been found to follow a power law [15]. This indicates that there is a permanent structural change by the UV-exposure process, which is irreversible. The AFM observation reveals that the surface relief is influenced by both laser power density and the presence of hydrogen. The structure compaction must be the result of the interaction between the UV energy and compositions in the glass. According to a theory proposed by Fokine [8], the UV-irradiation induces a photochemical reaction to form hydroxyl-groups under the presence of hydrogen. The periodic formation of hydroxyl-groups results in the periodic variation of the refractive index in the fibre core. The similar photochemical reaction would occur on the fibre surface due to the presence of hydrogen which may decompose the silicate glass molecular structure by breaking up the bonds between the silicon and oxygen atoms in the form of:

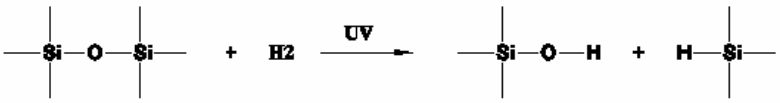

The appearance of Si-H and Si-O-H vibration bands was detected by Infrared (IR) spectra in the irradiated hydrogen-treated silica glass [16]. In hydrogen loaded germania-doped silica glass, upon UV-irradiation, various H-bearing species including H_2, SiOH, GeOH, SiH, GeH were identified in the IR measurements [17]. This evidence indicates that the interaction of UV energy and hydrogen alters the microstructure of glass by breaking the bonds and reforming new bonds and molecular groups. It is not clear if this change contributes to the structural compaction on the surface. However, the presence of hydrogen under the assistance of UV-laser energy may weaken the silicate molecular network which

leads to the lower FBG strength and the deeper surface relief pattern on the hydrogen-loaded fibres.

The permanent part of the structural change is likely to be induced directly by the UV-energy. The existence of photo-ablation may be assumed, as the amplitude of the surface modulation is closely related to the intensity of the UV-energy. Based on the densification model, standard telecom fibres with little photosensitivity can exclude the existence of photo-induced densified structure. The compaction surface relief pattern observed on the standard telecom fibre may result from the effect of photoablation which melts the silica glass and reforms local compact structures. The refractive index modulation remaining after thermal annealing may also be attributed to the photo-ablation effect as it brings irreversible structural change. In germanosilicate fibres without hydrogen loading, this photoablation may play a major role in the formation of the surface troughs. Both photoablation and chemical reaction may contribute to the surface relief pattern of hydrogenated fibres.

5 CONCLUSIONS

The primary surface of Ge-B-codoped fibres and standard telecom fibres with/without hydrogen loading was observed using AFM. The following conclusions can be made:

1) A periodic corrugation pattern induced by the UV exposure was observed on the surface of the fibres investigated. The surface relief period corresponds to that of the interference fringes generated by the phase mask.
2) The surface relief pattern exists only on the side of the fibre oriented toward the irradiating UV laser beam. This indicated that there is a photoinduced structural change on the surface of the cladding.

3) The amplitude of the corrugation in a range of 0.7-3.2 nm is dependent on both the intensity of the laser power and the presence of hydrogen. The spatial envelope of the amplitude of the corrugation is correlated with the intensity profile of the UV-beam.
4) Although the period of the surface corrugation mirrors to the period of the Bragg gratings in the core, the observation of the corrugation on the irradiated telecom fibre surface indicates no direct link between the surface relief and the change of refractive index in the core. Photo-ablation appears responsible for the surface compaction troughs.
5) Hydrogen loading the Ge-B codoped fibre prior to UV irradiation increased the amplitude of the corrugation with a value doubled that observed in the fibre not subjected to hydrogen loading.

ACKNOWLEDGEMENTS

The authors would like to give their sincere thanks to Ms Christine Kimpton for her skill and patience with the AFM investigation. Her enduring efforts made this paper possible.

REFERENCES

1. O. K. Hill, Y. Fuji, D. C. Johnson, and B. S. Kawasaki, Applied of Physics Letters, 32 (1978), p. 647-649.
2. P. J. Lemaire, R. M. Atkins, V. Mizrahi and W. A. Reed , Electron. Lett., 29 (1993), p.1191-1193.
3. D. P. Hand and S. J. Russell, " photoinduced refractive-index changes in germanosilicate fibres", Optics Letter, vol15 102-104, 1990.
4. H. G. Limberger, P. Y. Fonjallaz, R. P. Salathe and F. Cochet, Appl. Phys. Lett. 68(1996), p.3069-3071.
5. B. Poumellec, P. Guenot, I. Riant, P. Sansonetti, P. Niay, P. Bernage and J. F. Bayon, Optical Materials 4 (1995), p. 441-449
6. P. Cordier, J. C. Doukhan and E. Ferterin et al, Optical Communication, 11(1994), p. 269-275.

7. M. Douay and W. X. Xie et al, Journal of Lightwave Technology, 15 (1997), p. 1329-1342.
8. M. A. Fokine, Proceedings of the 46th International Wire & Cable Symposium, Philadelphia, 1997, p. 64-67.
9. P. J. Lemaire , Optical Engineering 30(1991), p.780-789.
10. R. Kashyap, Fibre Bragg Gratings, Academic Press, London, 1999. P.36
11. M. L. Dockney, S. W. James and R. P. Tatam, Meas. Sci. Technol., 7(1996), P. 445-448.
12. C. Y. Wei, S. W. James, C. C. Ye, R. P. Tatam and P. E. Irving, SPIE's 6th Annual International Symposium on Smart Materials and Structures, SPIE vol. 3670 (1999), p. 164-170.
13. C. Y. Wei, C. C. Ye, S. W. James. R. P. Tatam and P. E. Irving, The influence of hydrogen loading and the fabrication process on the mechanical strength of optical fibre Bragg gratings (submitted to Optical Materials).
14. S. R. Baker, H. N. Rourke, V. Baker and D. Goodchild, Journal of Lightwave Technology, 15 (1997), P.1470-1477.
15. S. Kannan, J. Z. Guo and P. J. Lemaire, Journal of Lightwave Technology, 15(1997), P.1478-1483
16. A. N. Trukhin, H. J. Fitting, T. Barfels and A. Von Czarnoski , Radiation Effects and Defects in Solids, 149 (1999), No. 1-4 pt 1, P.61-68
17. Q. Zeng, J. F. Stebbins, A. D. Heaney and T. Erdogan, Journal of Non-Crystalline Solids, 258 (1999), No1, P.78-91.

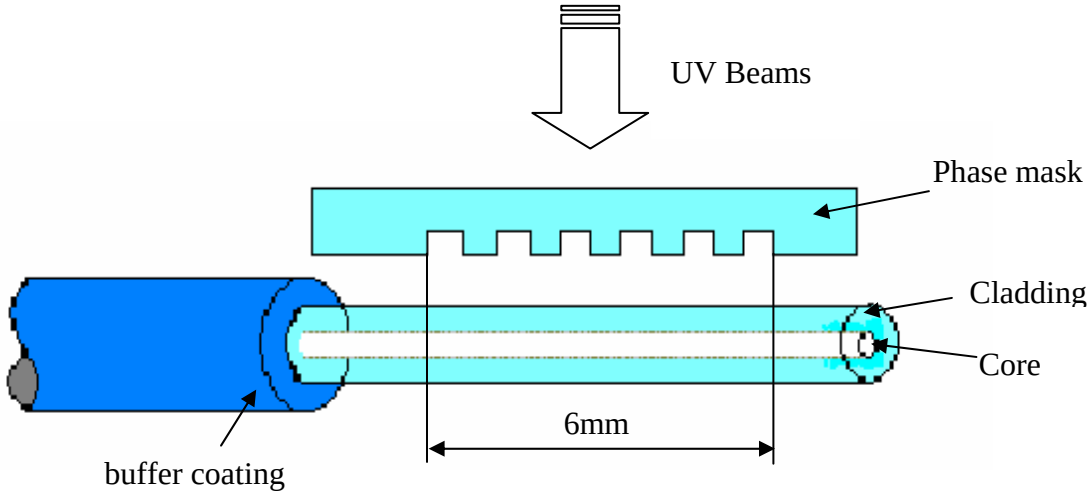

Fig. 1 Configuration of FBG fabrication using the phase mask technique

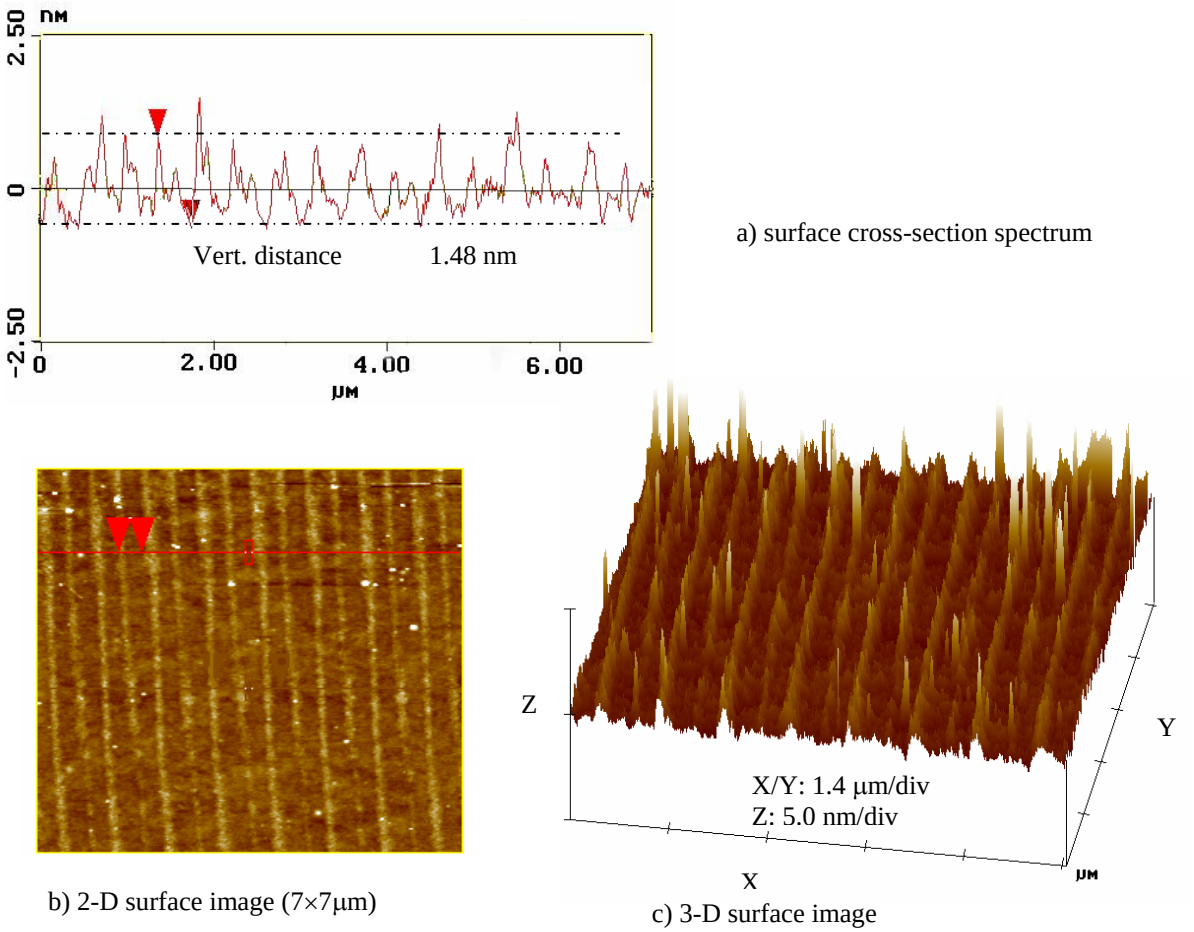

Fig. 2 AFM image of UV-irradiated surface for Ge-B codoped fibres under 2.4 W/cm^2 pulse power

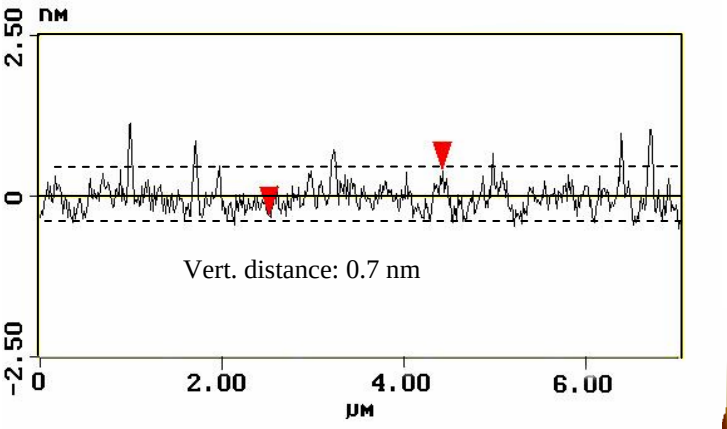

a) surface cross-section spectrum

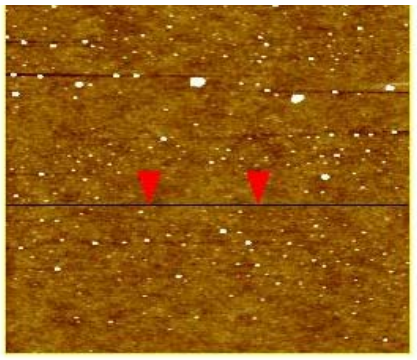

b) 2-D surface image (7×7μm)

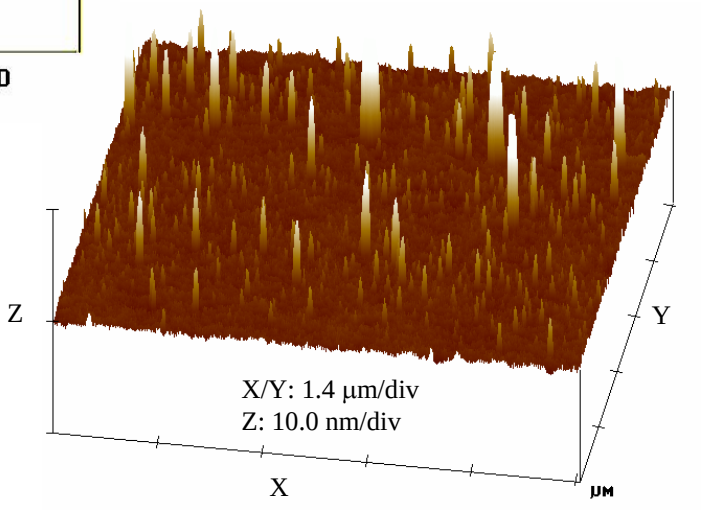

c) 3-D surface image

Fig. 3 Surface image of non UV-irradiated area on Ge-B codoped fibres

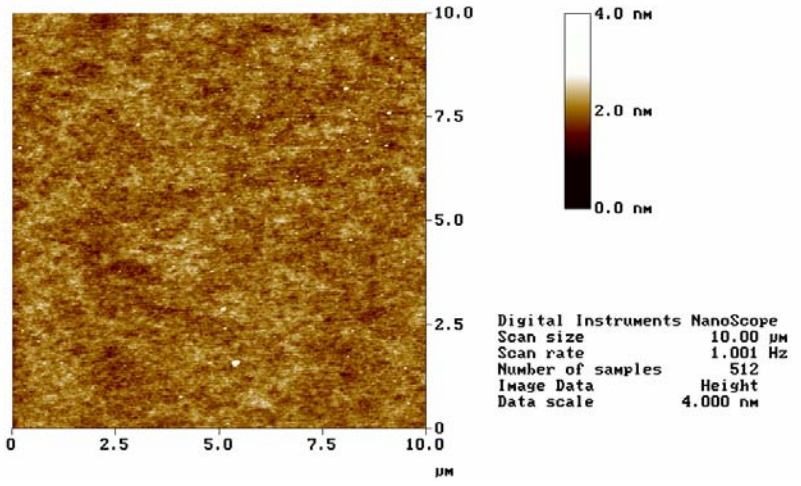

Fig. 4 Rear surface image of UV-irradiate region on Ge-B codoped fibre

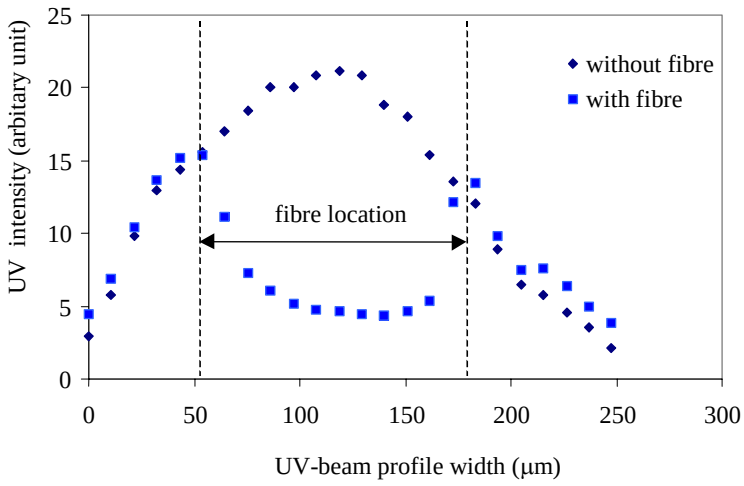

Fig. 5 UV intensity distribution behind an optical fibre and without the optical fibre

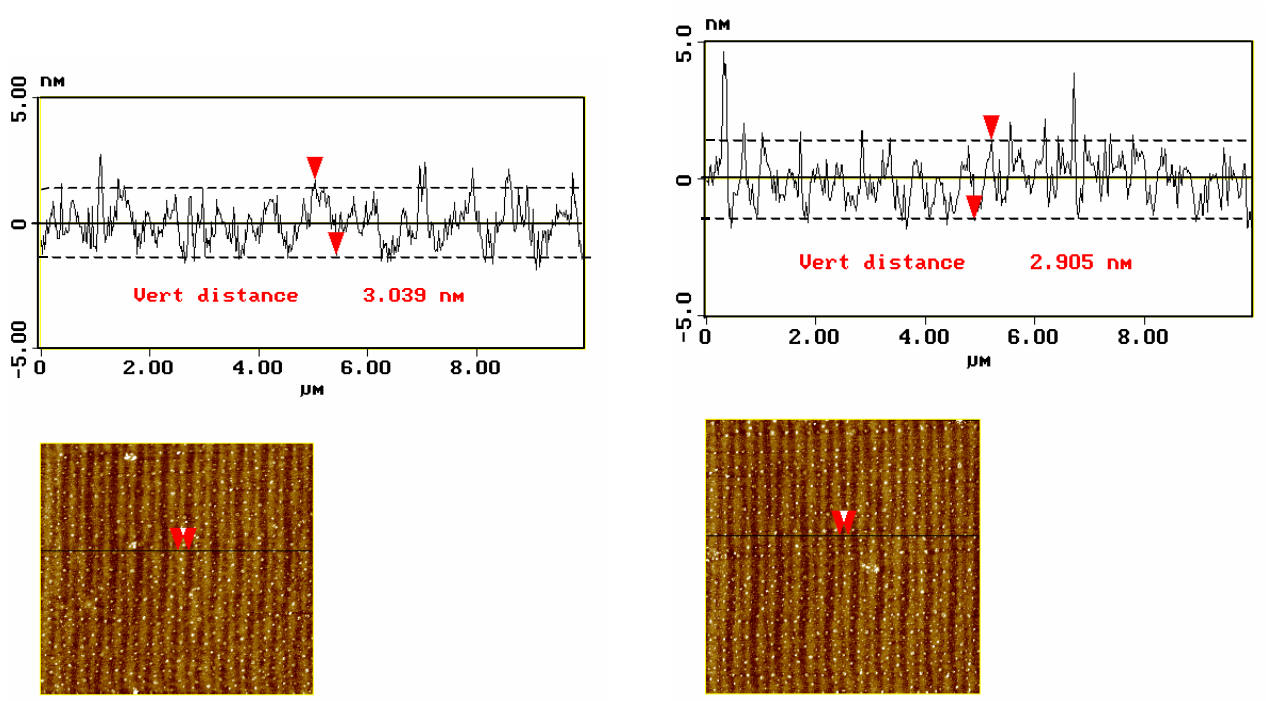

(a) at the centre of the irradiation (b) at 1.0 mm away from the irradiation centre

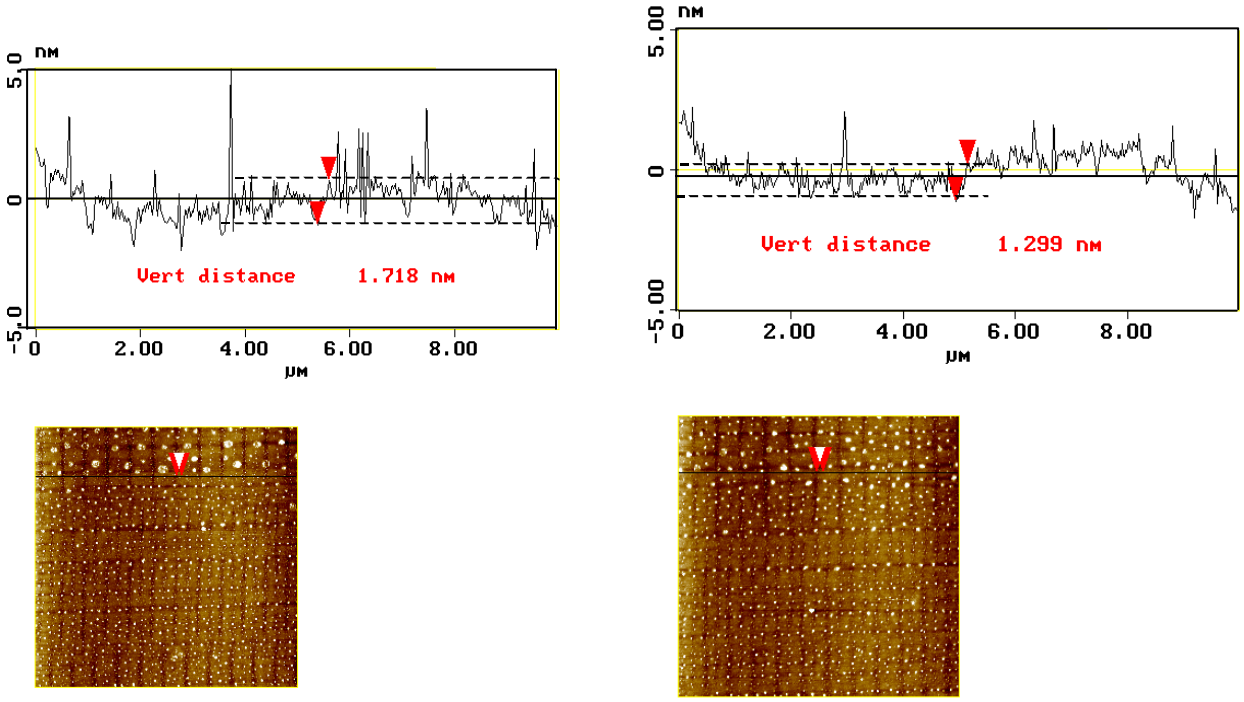

(c) at 2.0 mm away from the irradiation centre (d) at 3.0 mm away from the irradiation centre

Fig. 6. Surface images and cross-section spectrum analysis for the hydrogenated Ge-B codoped fibre under 2.0 W/cm^2 UV-irradiation (the surface area is: 10×10μm)

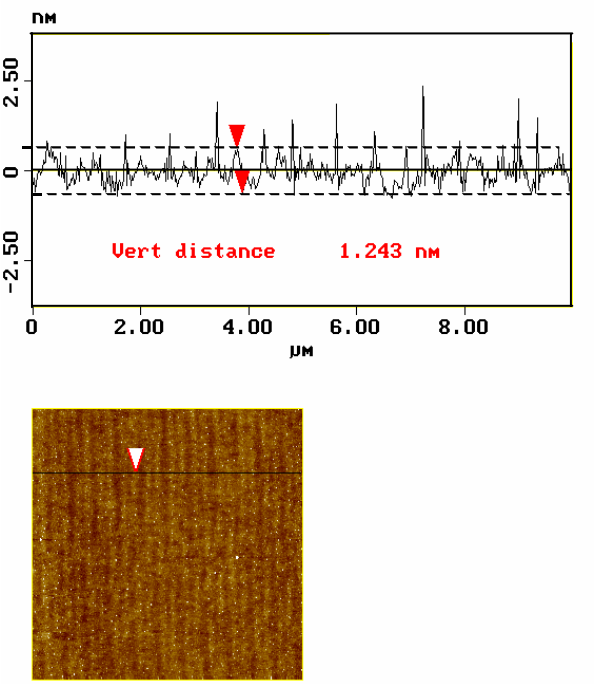

(a) at the irradiation centre

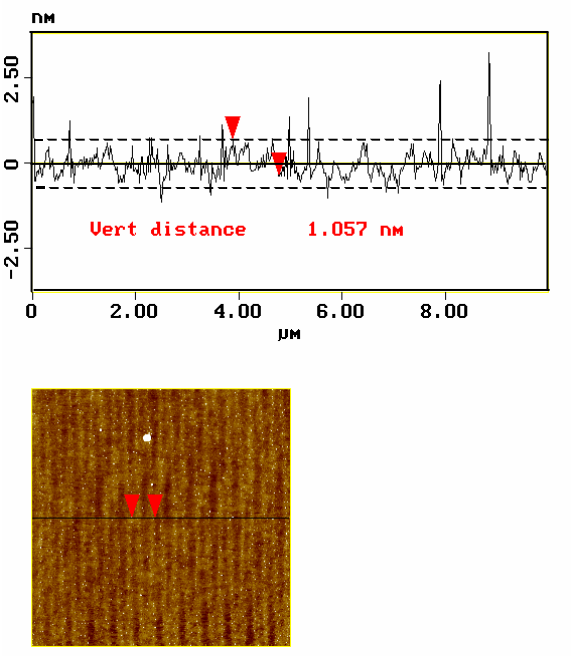

(b) at 1.0 mm away from the irradiation centre

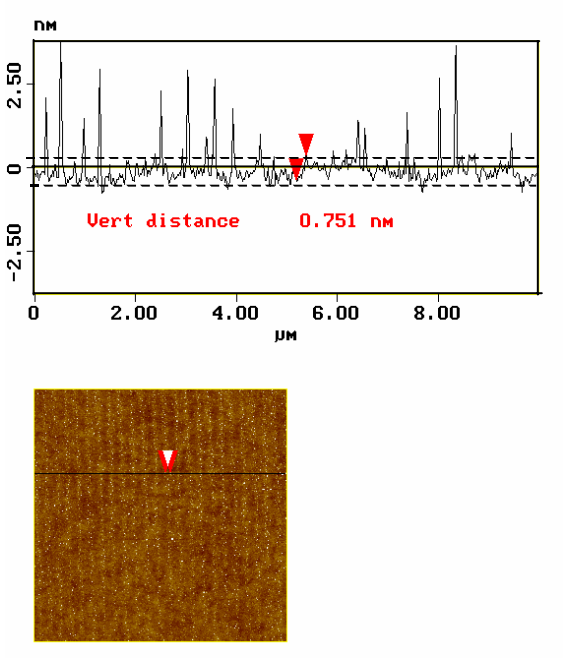

(c) at 2.0 mm away from the irradiation centre

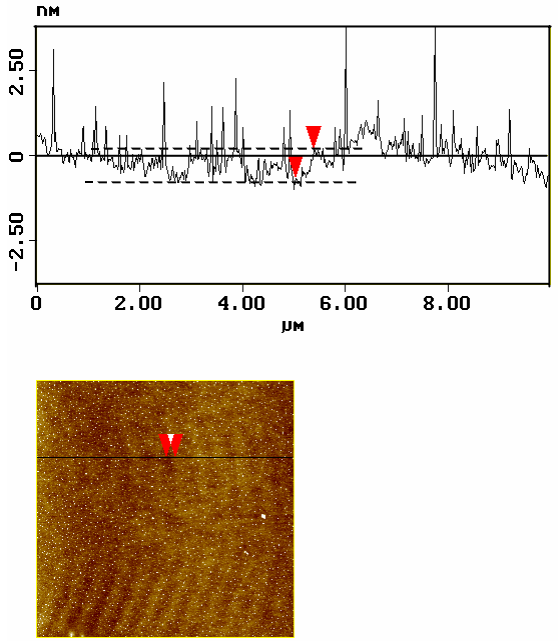

(d) at 3.0 mm away from the irradiation centre

Fig. 7 Surface images and cross-section spectrum analysis for the Ge-B codoped fibre under 2.0 W/cm^2 UV-irradiation (the surface area is: 10×10μm)

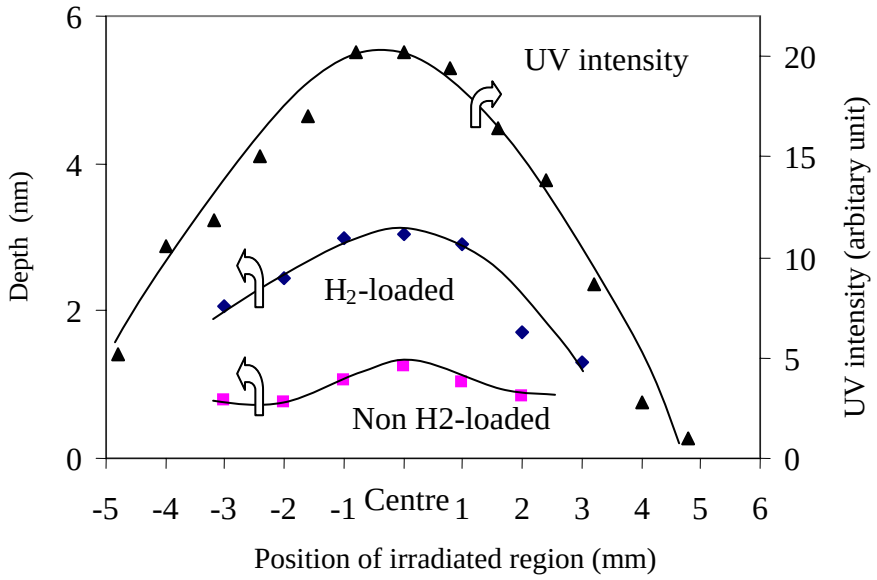

Fig. 8 Amplitude of surface corrugation vs. location of irradiated region on the Ge-B codoped with and without hydrogen loading, compared with UV intensity distribution over the irradiated region

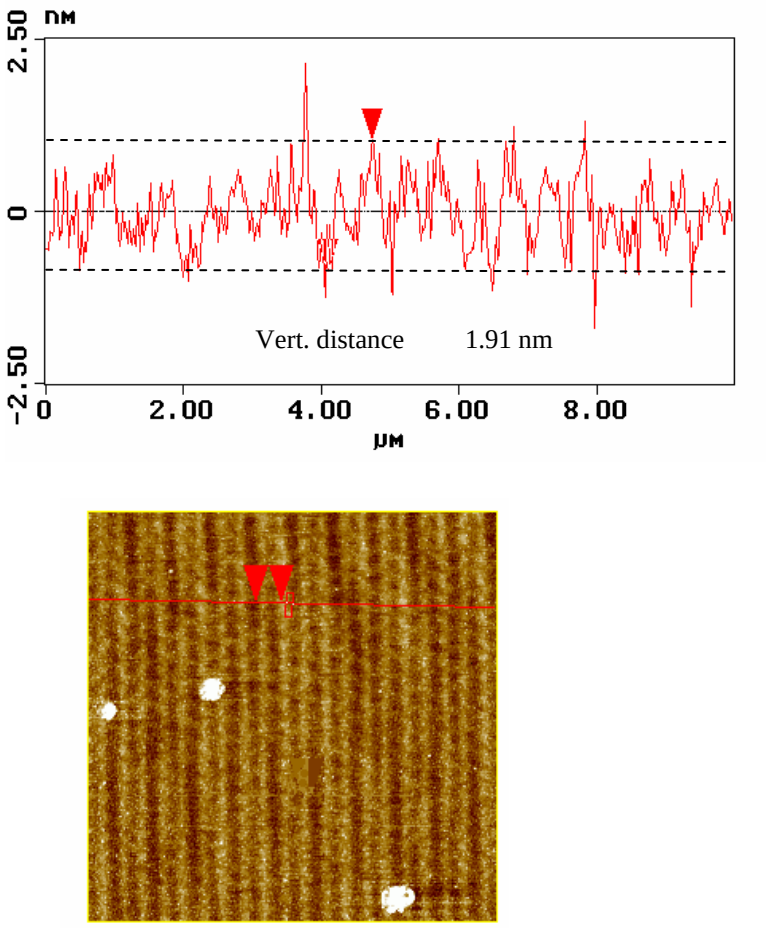

Fig. 9 Surface image (10×10µm) of irradiated standard telecom fibres under 2.4 W/cm^2 irradiation

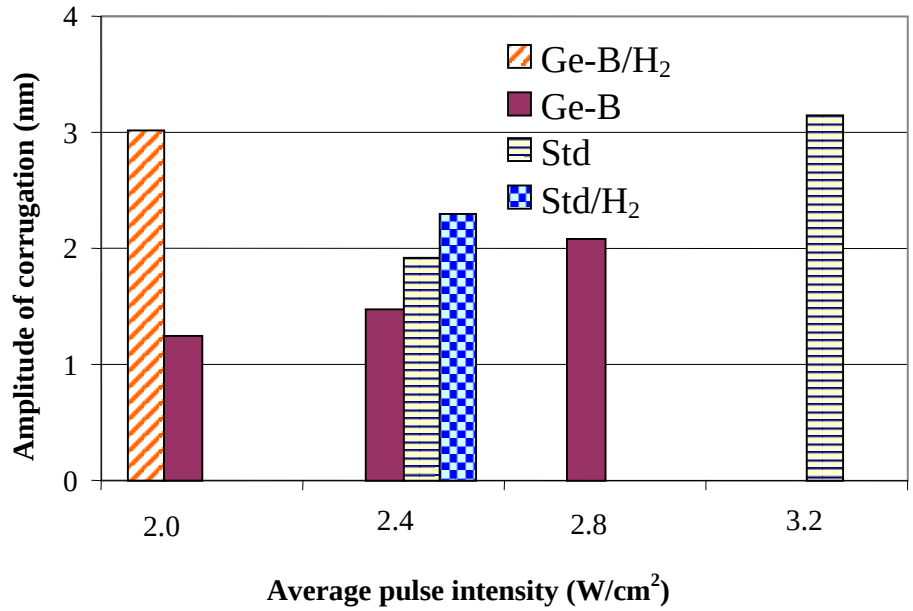

Fig. 10 Amplitude of surface corrugation vs fibre types and laser pulse power

Table 1: Fibre types and average UV-pulse intensity used in fibre Bragg grating fabrication

Fibre type\pulse power	2.0 W/cm^2	2.4 W/cm^2	2.8 W/cm^2	3.2 W/cm^2
Ge-B codoped	√	√	√	
Ge-B codoped/H_2-loaded	√			
Std fibres		√		√
Std/H_2-loaded		√		

* "√" represents that the AFM observation was performed on the fibre in that row which was irradiated under the laser power in that column